

MOTION ANALYSIS OF DEVELOPMENT OF WALL SLIP DURING DIE FLOW OF CONCENTRATED SUSPENSIONS

*Dilhan M. Kalyon, Halit Gokturk, Piraye Yaras and Birmur K. Aral
Highly Filled Materials Institute
Stevens Institute of Technology
Hoboken, NJ 07030*

ABSTRACT

A microscope and high speed motion analysis equipment were used to image the flow field occurring in die flow of concentrated suspensions following twin screw extrusion processing. The motion analysis revealed the development of a particle-free wall slip layer adjacent to the die wall. The nature of the slip layer is affected by the air content of the suspension. Air bubbles which are spherical away from the wall become ellipsoidal as they approach the wall and completely flatten into a thin film at the wall. The films of air momentarily stick to the die surface and then are dragged back into the bulk of the flowing suspension. The mechanism of slip layer formation and the role played by the entrained air have significant ramifications on the wall slip and rheological behavior of concentrated suspensions.

INTRODUCTION

Continuous processing technologies including single and twin screw extruders generally involve partially-full processing volumes. In partially full sections the material being processed such as the polymeric melt, blend, emulsion or suspension co-exists with air. Both the liquid and gas phases come into contact with a moving wall (screw surface). The location at which the solid moving wall comes into contact concomitantly with liquid and gas phases establishes the dynamic contact line. Such dynamic contact lines are also encountered in other industrially relevant flows including roll and tape-coating flows. The stability of the contact line depends on the balance of interfacial, inertial viscous and elastic forces [1]. When the dynamic contact line becomes unstable, the contact between the liquid and solid surface is lost and significant entrainment of the gas into the liquid phase takes place.

For example in roll-coating where a solid cylinder rotating with velocity U is partially immersed into a reservoir of Newtonian Liquid with

viscosity, μ , and surface tension, σ , the entrainment of air occurs when the capillary number Ca :

$$Ca = \frac{\mu U}{\sigma} \quad (1)$$

exceeds a critical value of 1.20 [2]. However, as the elasticity of the liquid phase increases (increasing first normal stress coefficient under steady shear), the critical capillary number increases [1].

On the other hand, when a moving surface enters into a pool of liquid at angle, α (tape coating) the critical Capillary number at which air entrainment occurs may depend on the entrance angle, α . The mechanisms of air entrainment have been reviewed [3] and they involve formation of large triangular air pockets for low viscosity fluids ($\mu < 0.1$ Pa-s) and entrainment through free air bubbles for higher viscosity fluids ($\mu > 0.2$ Pa-s).

In experimental studies aiming to investigate the devolatilization process in single screw extruders, Canedo [3] has investigated air entrainment occurring in a partially-full rectangular cavity, driven by a moving wall. The viscosity and surface tension values of the glycerol-water solutions investigated ranged from 0.005 to 12 Pa-s and 30-65 mN/m, respectively. The critical capillary number at which air entrainment occurred was found to depend on a "property group", γ , defined earlier by Bolton and Middleman [1]:

$$\gamma = \sigma \left(\frac{\rho}{g \mu^4} \right)^{1/3} \quad (2)$$

where ρ is fluid density and g is acceleration of gravity. Canedo [3] has reported critical Capillary numbers for air entrainment, Ca_{cr} in cavity driven flow as:

$$Ca_{cr} = 0.56 \gamma^{-0.66} \text{ for } 0.0004 < \gamma < 0.3$$
$$Ca_{cr} = 1.22 \gamma^{-0.19} \text{ for } 20 > \gamma > 0.3 \quad (3)$$

In subsequent studies specifically aiming at extrusion flows of polymer melts and concentrated

suspensions, Kalyon and co-workers [4-8] have shown that significant air entrainment occurs in partially-full sections of extrusion flows and affects the density and the rheological behavior of the polymer melt and concentrated suspensions.

In the flow of concentrated suspensions the formation of a binder-rich zone adjacent to the wall i.e., slip layer is observed [9-11]. Aral and Kalyon [7, 8] have shown that the slip velocities associated with the formation of the apparent slip layer and the rheological behavior of the bulk of the suspension upon wall slip collection are affected by the amount of air entrained into the suspension. However, the mechanisms and the role played by air entrainment on the development of wall slip layer formation were not elucidated in these earlier studies.

This present study aimed at determining how the air entrained into the suspension affects the development of the slip layer in extrusion/die flows of concentrated suspensions. The tools have included a transparent imaging window installed at a slit die surface, connected to a powerful microscope and high-speed camera based imaging system.

EXPERIMENTAL

Materials

The suspension of the study consisted of 60% by volume of poly(methyl methacrylate), PMMA, spheres incorporated into a blend of two silicone fluids. The PMMA spheres had a mean particle size of 47 μm , a refractive index of 1.491 and specific gravity of 1.17, and were available under the trade name of Lucite 4F from DuPont, Inc. The fluid phase consisted of a blend of phenyl methyl polysiloxane and penyl ethyl methyl modified poly(dimethyl siloxane) polymers available as Silicone Fluid 550 from Dow Corning, Inc., (83%) and L-42 from Union Carbide, Inc. (17%). The density of the blend was 1.06 g/cc and its refractive index was 1.491. Thus, the proper selection of the blend components allowed the approaching of the density and refractive index values of the binder and solid phases.

The close values of the densities of the solid and liquid phases of the suspension generated a near neutrally-buoyant suspension which eliminated sedimentation and buoyancy effects. The approaching of the refractive indices of the solid and liquid phases to each other facilitated easier imaging of the flow behavior of the suspension, although some of the individual particles could still be identified.

EQUIPMENT AND PROCEDURES

A slit die with a slit width of 2.5", slit length of 4" and a slit gap of 0.2" was connected to a Baker-Perkins 50.8 mm co-rotating twin screw extruder as shown in Figure 1. Dynisco pressure transducers were installed flush with the die wall, at 1" length intervals along the die. The microscope which was installed above the slit die/imaging window consisted of a Bausch and Lomb body (2505 UD), a Melles-Griot bright field 10X eyepiece and a Leitz objective with 20X magnification. The microscope objective was selected to have a relatively large numerical aperture of 0.33 and thus to provide a relatively narrow depth of field. The optical window was machined out of borosilicate glass and had an aperture of 1 mm by 1.2 mm. A GaAlAs laser with an emission wavelength of 788 nm (Model LN9705P from Matsushita Corporation) was used for illumination.

The shallow depth of field of the microscope coupled with the monochromatic illumination provided by the laser source allowed sectioning of the image in the depth direction as a function of distance from the fluid/optical wall interface. The accuracy of the depth resolution of the optical set-up was initially tested by imaging the markings of a stationary reticle. The reticle contained well-defined consecutive markings. The reticle was tilted at various angles by means of a rotational micropositioner to determine the resolution of the depth of field settings which was found to be within $\pm 20 \mu\text{m}$. The optical system also allowed the determination of particle velocities from the particles which were identified and the speckle flashes emitted by the individual particles.

The motion study was carried-out using a high-speed motion analyzer available from Kodak i.e., Ekta Pro Hi-Spec analyzer. This analyzer incorporates a high-speed digitizer which can record up to 1,000 full frames per second and provides immediate playback on a video monitor. For the analysis of the collected images, Automatix II hardware and software were used.

RESULTS AND DISCUSSION

Typical images collected using a recording speed of 500 frames/s and at a suspension volumetric flow rate of $2.4 \times 10^{-6} \text{ m}^3/\text{s}$ at 25°C are shown in Figure 2a-c. These images were collected upon the focusing of the microscope at the wall and fluid interface and they indeed indicate that a particle free zone develops adjacent to the wall during the pressure induced flow of the concentrated suspension through the slit die.

The nature of the particle free zone changes as a function of time principally influenced by the role played by the air content of the suspension. Air bubbles within the bulk of the suspension were observed to be spherical with a typical diameter of $97 \pm 15 \mu\text{m}$ (confidence intervals according to Student's-t-distribution) when they were located away from the wall area. However, upon approaching the wall, the air bubbles were distorted into ellipsoidal shapes with their main axis elongated in the flow direction.

The air bubbles came into direct contact with the solid interface in a cyclic fashion. The bubbles were seen to flatten at the solid interface and glide and roll over the interface. The air film thus formed at the wall typically momentarily sticks to the wall for a duration of about $30 \text{ ms} \pm 10 \text{ ms}$ upon which it is dragged and removed from the solid surface. The time interval of the coating of the solid/fluid interface by consecutive spreading and film formation occurred over a broad time range with values varying between 40 ms to 600 ms. The mean time interval values determined from different runs were within $325 \pm 107 \text{ ms}$. It should be emphasized that the collection of such imaging data was only possible due to the availability of the high-speed cinematography tool i.e., the Kodak motion analyzer operated at 500 frames/second. Conventional video equipment which run around 30 frames/second would not have resolved the formation of the slip layer and the role played by air films in the development of this particle-free region.

The typical distribution of velocity of the suspension in the vicinity of the solid wall is shown in Figure 3. The discrete points represent the velocity values of individual particles observed to flow at different depth locations away from the wall. The typical 95% confidence intervals determined according to Student's-t-distribution are also indicated. The solid particles found adjacent to the slip layer are found to move at velocities in the range of 2.5-3 mm/s. However, although the formation of air films at the wall could be identified with certainty, the location of the particles and, hence, their velocities are subject to the uncertainty of $\pm 20 \mu\text{m}$ in depth measurement.

In our earlier studies [6, 9, 10], we have shown that the slip velocity, U_s , generally varies linearly with the wall shear stress, τ_w , i.e.,

$$U_s = \beta \tau_w \quad (4)$$

A quick order-of-magnitude calculation reveals that this slip velocity range of 2.5-3 mm/s is within the range of values expected for concentrated suspensions filled with 60% by volume solids, i.e., smaller than or equal to 10 mm/s.

These results further support our earlier findings on the role played by air entrainment on the wall slip and rheology of concentrated suspensions [5, 6, 8]. In these earlier studies, it was shown that the reduction of the air content of a concentrated suspension increases its shear viscosity and decreases its wall slip velocity. For example, a suspension consisting of a poly(butadiene-acrylonitrile-acrylic acid) binder and 63% by volume solid glass spheres (with a narrow size distribution of solid particles, comparable to the size distribution of present study) gave rise to a Navier's slip coefficient, β , of about $7.4 \times 10^{-5} \text{ mm}/(\text{Pa}\cdot\text{s})$ when the suspension was prepared without the application of vacuum in the extruder. The Navier's slip coefficient decreased to $5.4 \times 10^{-5} \text{ mm}/(\text{Pa}\cdot\text{s})$ when the air content of the suspension was reduced upon devolatilization in the extruder. Clearly, the increase in the Navier's slip coefficient is associated with the enhanced formation of air films at the wall which shall increase the slip velocity of the binder-rich zone found adjacent to the air film. This occurs because at the flat air and fluid interface the shearing stress vanishes i.e.,:

$$\bar{n} \cdot \underline{\underline{\tau}} \cdot \bar{t} = 0 \quad (5)$$

where \bar{n} is the unit vector pointing outward normal from the wall, \bar{t} is the unit vector tangent to the surface and $\underline{\underline{\tau}}$ is the stress tensor for the binder flowing in the slip layer. It can be expected that a greater portion of the wall surface would be covered with the air film upon the increase of the air concentration in the suspension, thus increasing the Navier's slip coefficient. The cyclic nature of the air film formation at the surface which was observed to occur at a typical frequency of 3 per second should give rise to oscillations in die pressure at the same frequency. However, our pressure measurement technique was not sensitive enough to document this expected stick-slip effect.

The findings of this study also have significant ramifications on other processing flows including roll and tape coating flows. Modeling of the contact line reveals that a singularity develops at the dynamic contact line where the velocity is discontinuous and stresses go to infinity [12, 13]. The traditional method of removing this singularity is to assume a Navier's wall slip condition [14-16].

$$\beta(\bar{n} \bar{t} : \underline{\underline{\tau}}) = \bar{t} \cdot (\bar{U} - \bar{U}_w) \quad (7)$$

where \bar{U} is the fluid velocity at the wall and \bar{U}_w is the wall velocity. For one-dimensional flows the wall slip condition is given by Equation 4. It is very likely that the mechanisms of wall slip revealed by

equally applicable to free-surface flows of a wide class of materials where, as noted earlier, the entrainment of air into the fluid becomes readily detectable even with conventional experimental techniques.

Thus, the critical capillary number represented by Equation 3 only represents a limit at which the air entrainment into the liquid becomes so wide-spread that it becomes noticeable even with naked eye. The application of the microscopy/high-speed imaging techniques of this present study to the investigation of such free surface flows can indeed reveal the development of a slip layer through the formation of air films at the interface, similar to what is observed here, to occur below the detection limit of the naked eye or conventional imaging techniques. The slip layer may exist even at the smallest capillary numbers. This indicates that the numerical convenience, i.e., assumption of a wall slip condition, which removes the singularity at the dynamic contact line, is rooted in the actual wall slip phenomenon.

ACKNOWLEDGMENTS

This research has been sponsored by BMDO/IST as managed by Dr. Richard S. Miller of ONR (grant number N00016-86-K-0620), for which we are grateful. The content of the information does not necessarily reflect the position or the policy of the Government, and no official endorsement should be inferred.

REFERENCES

1. Bolton, B. and S. Middleman (1980), "Air Entrainment in a Roll Coating System," *Chem. Eng. Sci.*, 35, pp 597-601.
2. Wilkinson, W.L. (1975), "Entrainment of Air by a Solid Surface Entering a Liquid/Air Interface," *Chem. Eng. Sci.*, 30, pp 1227-1230.
3. Canedo, E. L., "Flow and Mass Transfer in Driven Cavities with a Free Surface," Ph.D. Thesis, U. of Delaware (1985).
4. Kalyon, D.M., C. Jacob and P. Yaras (1991), "An Experimental Study of the Degree of Fill and Melt Densification in Fully-intermeshing, Co-rotating Twin Screw Extruders," *Plast. and Rubber Comp. Proc. and Appl.*, 16, pp. 193-200.
5. Kalyon, D.M., R. Yazici, C. Jacob, B. Aral and S. W. Sinton (1991), "Effects of Air Entrainment on the Rheology of Concentrated Suspensions during Continuous Processing," *Polym. Eng. Sci.*, 31, pp. 1386-1392.
6. Aral, B., D. M. Kalyon and H. Gokturk (1992), "The Effects of Air Incorporation in Concentrated Suspension Rheology," *SPE ANTEC Tech. Papers*, 38, pp. 2448-2451.
7. Aral, B. and D. M. Kalyon (1993), "Time-Dependent Development of Wall Slip in Shear Flows of Concentrated Suspensions," *SPE ANTEC Technical Papers*, 39, pp. 2607-2610.
8. Aral, B. and D. M. Kalyon, "Rheology and Extrudability of Very Concentrated Suspensions: Effects of Vacuum Imposition," submitted to *Plast. and Rubber Comp. Proc. and Appl.*, 1994.
9. Yilmazer, U. and D. M. Kalyon (1989), "Slip Effects in Capillary and Parallel Disk Torsional Flows of Highly Filled Suspensions," *J. Rheology*, 33, pp. 1197-1212.
10. Kalyon, D.M., P. Yaras, B. Aral and U. Yilmazer (1993), "Rheological Behavior of Concentrated Suspensions: A Solid Rocket Fuel Simulant," *J. Rheology*, 37, pp. 35-53.
11. Aral, B. and D. M. Kalyon (1994), "Effects of Temperature and Surface Roughness on Time-Dependent Development of Wall Slip in Torsional Flow of Concentrated Suspensions," *J. of Rheol.*, 38, pp. 957-972.
12. Moffatt, H.K. (1964), "Viscous and Resistive Eddies Near a Sharp Corner," *J. Fluid Mech.*, 18, pp. 1-18.
13. Huh, C. and L.E. Scriven (1971), "Hydrodynamic Model of Steady Movement of a Solid/Liquid/Fluid contact Line," *J. Colloid Interf. Sci.*, 35, pp. 85-101.
14. Hocking, L.M. (1977), "A Moving Fluid Interface: The Removal of the Force Singularity by a Slip Flow," *J. Fluid Mech.*, 79, pp. 209-229.
15. Silliman, W.J. and L.E. Scriven (1980), "Separating Flow Near a Static Contact Line: Slip at a Wall and Shape of Free Surface," *J. Comp. Phys.*, 34, pp. 287.
16. Kistler, S.F. and L.E. Scriven (1983), "Coating Flows," in *Computational Analysis of Polymer Processing*, J.R.A. Pearson and S.M. Richardson, Eds., London, Applied Science, pp. 243-299.

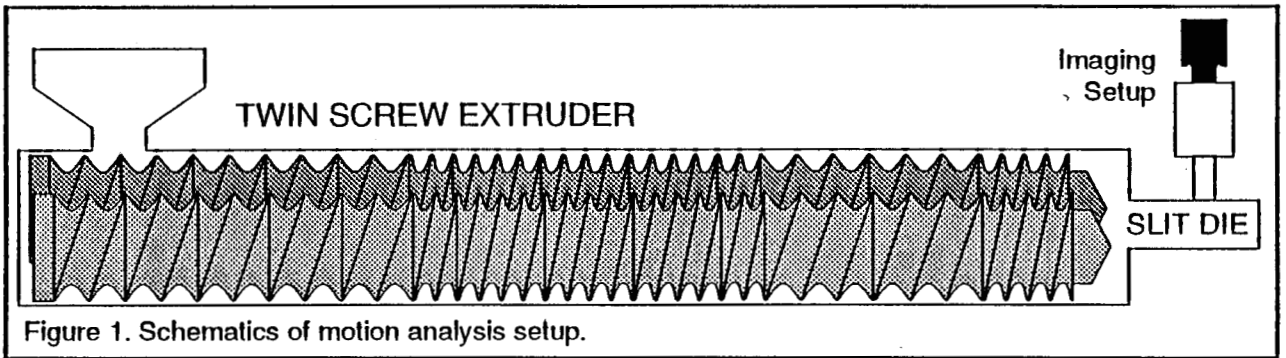


Figure 1. Schematics of motion analysis setup.

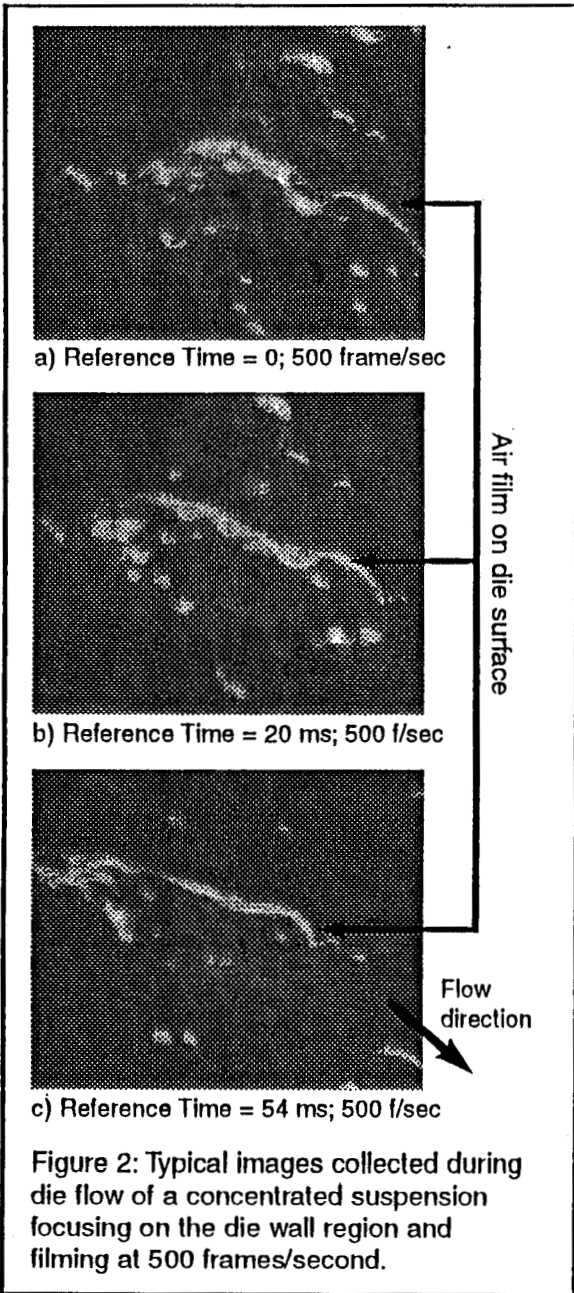


Figure 2: Typical images collected during die flow of a concentrated suspension focusing on the die wall region and filming at 500 frames/second.

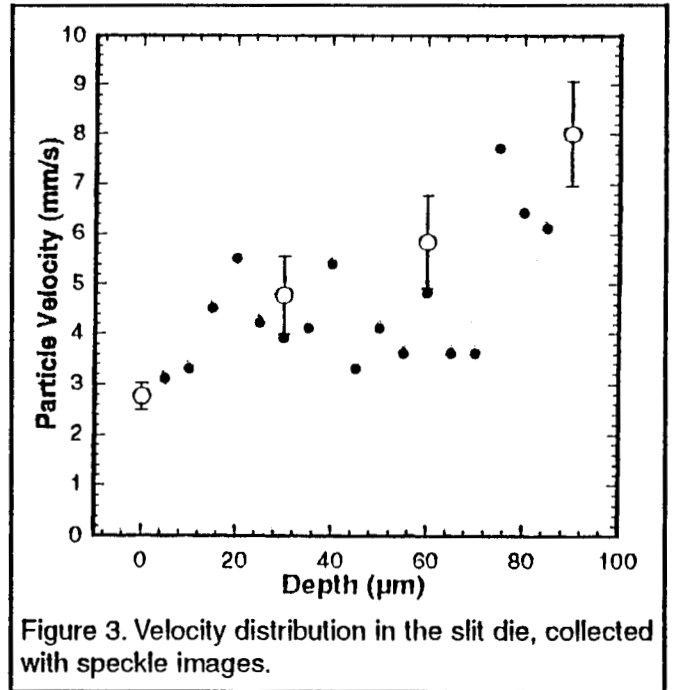


Figure 3. Velocity distribution in the slit die, collected with speckle images.